

The process $e^+e^- \rightarrow \pi^+\pi^-\pi^0$ in the energy range $2E_0 = 1.04\text{--}1.38$ GeV

M.N.Achasov, V.M.Aulchenko, S.E.Baru, K.I.Beloborodov, A.V.Berdyugin,
A.V.Bozhenok, A.D.Bukin, D.A.Bukin, S.V.Burdin, T.V.Dimova, S.I.Dolinsky,
V.P.Druzhinin, M.S.Dubrovin, I.A.Gaponenko, V.B.Golubev, V.N.Ivanchenko,
I.A.Koop, P.M.Ivanov, A.A.Korol, S.V.Koshuba, E.V.Pakhtusova,
E.A.Perevedentsev, A.A.Salnikov, S.I.Serednyakov*, V.V.Shary, Yu.M.Shatunov,
V.A.Sidorov, Z.K.Silagadze, A.N.Skrinsky, Y.V.Usov, A.V.Varganov,
A.V.Vasilyev, Yu.S.Velikzhanin

Budker Institute of Nuclear Physics, Novosibirsk State University,
Novosibirsk, 630090, Russia

Abstract

In the experiment with the SND detector at VEPP-2M e^+e^- collider the process $e^+e^- \rightarrow \pi^+\pi^-\pi^0$ was studied in the energy range $2E_0$ from 1.04 to 1.38 GeV. A broad peak was observed with the visible mass $M_{vis} = 1220 \pm 20$ MeV and cross section in the maximum $\sigma_0 \simeq 4$ nb. The peak can be interpreted as a ω -like resonance $\omega(1200)$.

PACS: 13.25.-k; 13.65.+i; 14.40.-n

Keywords: e^+e^- collisions; Vector meson; Detector

*e-mail:serednyakov@inp.nsk.su; FAX: +7(3832)342163

Introduction. The process $e^+e^- \rightarrow \pi^+\pi^-\pi^0$ dominates in the isoscalar part of the total cross section of e^+e^- annihilation into hadrons. In the low energy region $2E_0 \sim 1$ GeV this process is measured with a relatively high accuracy $\sim 3\%$ only in the vicinity of isoscalar resonances $\omega(783)$ and $\phi(1020)$. In the region above $\phi(1020)$ there are data from detectors ND [1] and DM2 [2], but the statistics in these experiments is quite small. In the Tables [3] the $\omega(1420)$ and $\omega(1600)$ states are listed, but their parameters, based entirely on DM2 measurements of the processes $e^+e^- \rightarrow 3\pi, \omega\pi\pi$, are not well established.

Experiment. In this work the process

$$e^+e^- \rightarrow \pi^+\pi^-\pi^0 \quad (1)$$

was studied in the energy range $2E_0 = 1.04 - 1.38$ GeV at the VEPP-2M e^+e^- collider with SND detector [4]. The integrated luminosity in the experiment [5] is $L = 6.1\text{pb}^{-1}$. In the study of the process (1) the main background comes from the processes

$$e^+e^- \rightarrow \pi^+\pi^-\pi^0\gamma, \quad (2)$$

$$e^+e^- \rightarrow \pi^+\pi^-\pi^0\pi^0, \quad (3)$$

$$e^+e^- \rightarrow e^+e^-\gamma\gamma. \quad (4)$$

The radiative process (2) with emission of hard photons particularly by initial electrons is a source of background in the vicinity of $\phi(1020)$, where its cross section is determined by intermediate $\phi\gamma$ state decay further into $\pi^+\pi^-\pi^0\gamma$. The process (3) gives contribution due to merging of showers in the calorimeter, loss of photons and errors in events reconstruction.

Events Selection. To select events of the process (1) and suppress the background, the following cuts were applied:

1. Two charged particle tracks and two photons are found in an event,
2. Particle angle with respect to the beam is $\theta > 27^\circ$,
3. The total energy deposition ΔE in is $0.9E_0 < \Delta E < 1.8E_0$,
4. The spatial angle ψ_{12} between charged particles is $\psi_{12} < 160^\circ$,
5. The reconstructed by kinematic fitting energies of two charged pions are restricted by the cuts $E_1 < 0.75 \cdot E_0$ and $E_2 < 0.65 \cdot E_0$,
6. The minimal photon energy is $E_{\gamma,min} > 0.1 \cdot E_0$,
7. The photon quality parameter is $\zeta < 30$,
8. The kinematic fit parameter is $\chi_{3\pi} < 10$.

The photon quality parameter ζ describes the likelihood of a hypothesis, that given transverse energy profile of a cluster in the calorimeter can be attributed to a single photon [6]. The parameter $\chi_{3\pi}$ describes the degree of energy-momentum balance in an event under assumption of $\pi^+\pi^-\pi^0$ final state. The cut 8 suppresses all background processes, while other cuts are efficient against the processes (4) and (3).

Data analysis. The total of $N=6550$ events were selected in 34 energy points after applying selection cuts. The visible cross section $\sigma_{vis} = N/L - \sigma_B$, obtained after imposing all selection cuts, is shown in the Fig.1. In the definition of σ_{vis} , L is an integrated luminosity in a given energy point, measured by means of Bhabha scattering process, N is the number of selected events, and σ_B is the contribution from the background processes (3) and (4). The value of σ_B , estimated from simulation, does not exceed 5%. The solid line in Fig.1 shows the vector meson dominance model (VMD) prediction for the processes (1) and (2) with contributions of $\omega(783)$ and $\phi(1020)$ states only. One can see, that at $2E_0 > 1100$ MeV, the measured cross section significantly exceeds VMD prediction. An enhancement in the visible cross section near 1200 MeV is seen.

The detection efficiency ϵ for the pro-

cess (1) was calculated using simulated events of the processes (1) and (2). The obtained value of ϵ varies from 12% to 14% in the energy range $2E$ from 1040 to 1380 MeV. It was found, that for the process (2) the detection efficiency strongly depends on the energy of the radiative photon ω and due to the simple relation: $\omega \simeq 2E_0 - M_\phi$ — on the beam energy. One could see from Fig.2, that events with $\omega > 100$ MeV do not pass the cuts. Thus at the beam energy $2E > 1120$ MeV the $\phi\gamma$ intermediate state in the process (2) does not contribute into σ_{vis} and the detection efficiency is determined mainly by the process (1).

To determine the $\pi^+\pi^-\pi^0$ production cross section the following expression was used:

$$\sigma_{vis} = \epsilon \cdot \sigma_0 \cdot (1 + \delta), \quad (5)$$

where σ_0 is the cross section of the process (1), δ is a radiative correction [7]. The radiative correction sharply depends on the energy, decreasing from ~ 50 at $2E_0 = 1040$ MeV to ~ 0.2 at $2E_0 = 1200$ MeV. All variables in Eq.5 are considered as functions of energy. The Born cross section σ_0 of the process (1), obtained from the Eq.5 is shown in Fig.3 and listed in the Table 1. The broad peak is seen with effective mass $M_{eff} \simeq 1200$ MeV. One can see, that the measured cross section agrees with the previous ND data [1] and recent CMD-2

measurements at $2E < 1050$ MeV [10]. In simulation of the processes (1) and (2) the cross section energy dependence was taken from the Table 1. The measured cross section σ_0 is plotted in a wider energy range in the Fig.4 together with DM2 data [2]. One can see, that DM2 cross section at higher energy well matches SND data.

The systematic error of the measured cross section includes following contributions:

- error in detection efficiency estimation $\sim 10\%$,
- error in background subtraction from the processes (3), (4) $\sim 3\%$,
- error in background subtraction from the radiative process (2).

The last error is estimated to be $\sim 3\%$ at $2E_0 > 1150$ MeV, but at lower energy it grows up to $\sim 50\%$. The total systematic error at $2E_0 > 1150$ MeV is estimated to be 12%.

The structure of the 3π final state was analysed in our earlier work [5] where it was found, that $\rho\pi$ intermediate state dominates there. Moreover, manifestation of $\rho - \omega$ interference in the final 3π state, caused by $e^-e^+ \rightarrow \omega\pi^0$, $\omega \rightarrow \pi^-\pi^+$ process, predicted in [8], was observed. The immediate consequence of this effect is possible change in mass spectra and cross sec-

tion of the process (1) by $\sim 10\%$. In the present work the process (1) was simulated with the only $\rho\pi$ intermediate state.

Fitting of the cross section. To test energy dependence of the cross section on possible deviations from VMD model, we fitted our data together with the data obtained in other experiments outside the interval $2E = 1.04 \div 1.38$ GeV: ND[1], CMD-2[11], and DM2[2].

The following expression from the works [9, 10] was used for approximation of the cross section as a sum of resonances:

$$\sigma_0(e^+e^- \rightarrow \pi^+\pi^-\pi^0) = \frac{W_{\rho\pi}(s)}{s^{3/2}} \cdot \left| \sum_V \sqrt{\frac{\sigma_V \cdot m_V^3}{W_{\rho\pi}(m_V^2)}} \cdot \frac{e^{i\phi_V} \Gamma_V m_V}{s - m_V^2 - im_V \Gamma_V(s)} \right|^2, \quad \sigma_V = \frac{12\pi B_{Vee} B_{V\rho\pi}}{m_V^2}. \quad (6)$$

Here $W_{\rho\pi}(s)$ is a phase space factor of the final state. The following 4 resonances were included in the fitting: $\omega(783)$, $\phi(1020)$, $\omega(1600)$, and an additional ω -like state $\omega(1200)$ with its parameters set free. The energy dependence of Γ_V was taken into account only for two lightest states $\omega(783)$ and $\phi(1020)$. The parameters of $\omega(783)$ and $\phi(1020)$ and their errors were taken from PDG Tables [3]. The phases $\omega(783)$ and $\phi(1020)$ were fixed: $\phi_{\omega(783)} = 0$; $\phi_{\phi(1020)} = \pi$.

To evaluate parameters of the $\omega(1600)$ -resonance independently the $e^+e^- \rightarrow \omega\pi\pi$ production cross section, measured by DM2

[2], was fitted separately with expression similar to Eq.6, giving $M(\omega(1600)) = 1643 \pm 14$ MeV, $\Gamma(\omega(1600)) = 272 \pm 29$ MeV and $\sigma_{max} = 3.1 \pm 0.3$ nb. These values statistically agree with the PDG Tables parameters of $\omega(1600)$, therefore they were used in final fitting.

Four possible choices of phases $\phi_{\omega(1200)}$ and $\phi_{\omega(1600)}$: $\phi_{\omega_i} = 0, \pi$, corresponding to constructive and destructive interference, were considered. We found that the fit with $\phi_{\omega(1200)} = 0$ contradicts CMD-2 data, while the fit with equal $\phi_{\omega(1200)}$ and $\phi_{\omega(1600)}$ phases disagrees with DM2 data. The $\omega(1600) \rightarrow 3\pi$ decay in the latter case is not seen. The fit with $\phi_{\omega(1200)} = \pi$ and $\phi_{\omega(1600)} = 0$, satisfies all data. The data and resulting fitting curve for this case are shown in Figs.3,4,5. The $\chi^2/N.D.$ parameter for SND data is 25/34 ($P(\chi^2) = 87\%$). The main result of the fitting is that a new state, referred to as $\omega(1200)$, was found instead of $\omega(1420)$. The fit parameters of $\omega(1200)$ and $\omega(1600)$ states are listed in the Table 2. The systematic error $\sim 12\%$ is not included into mass and width, but it is included into the cross section σ_{max} and electron width.

Fitting with other three phase choices, giving poor values of $P(\chi^2) \sim 5\%$, yields $\omega(1200)$ mass M_{eff} , varying within $1170 \div 1250$ MeV and the width Γ_{eff} from 190 to

550 MeV. The optimum interference phases cannot be derived from only SND data, requiring additional data from outside the interval $2E = 1.04 - 1.38$ GeV obtained in other experiments. Thus the interference phases and $\omega(1200)$ parameters may change if these data change. Moreover in models with strong energy dependence of resonance widths the $\omega(1200)$ parameters are expected to be different too.

Fitting with a single resonance above $\phi(1020)$ gives nothing new, because this case coincides with already mentioned fit with equal phases $\phi_{\omega(1200)} = \phi_{\omega(1600)}$ giving poor $P(\chi^2)$.

Using the cross section in the $\omega(1600)$ maximum we obtained the following ratio:

$$B(\omega(1600) \rightarrow 3\pi)/B(\omega(1600) \rightarrow \omega\pi\pi) = 0.17 \pm 0.05.$$

Discussion. To fit the data above $\phi(1020)$ we used simple Breit-Wigner model, which gives resonance parameters (mass, width,..) close to the visible ones. This approach facilitates the comparison of data from different experiments. But we keep in mind, that in other models, e.g. in models with strong width dependence on energy, the mass and width can differ significantly (> 100 MeV) from their apparent values.

If our explanation of the cross section enhancement as a new $\omega(1200)$ state is confirmed, the question of its nature arises. It

could be either first radial excitation 2^3S_1 or an orbital excitation (D-wave) 1^3D_1 of $\omega(783)$. Such excited states are known for $\rho(770)$: $\rho(1450)$ and $\rho(1600)$. But here we encounter the problem of $\omega(1200)$ mass, which is considerably lower than masses of its isovector partners. It is worth mentioning, that the $\rho(1450)$ and $\rho(1600)$ parameters are not well established either. So, new data as well as more advanced analysis of the existing data are needed. In the energy range $2E_0 < 1.4$ GeV in the nearest future new data are expected from two VEPP-2M detectors — SND[4] and CMD-2[11] for many channels of e^+e^- annihilation into hadrons: 2π , 3π , 4π , 5π , $K\bar{K}$, etc.

Conclusions. The cross section of the process $e^+e^- \rightarrow \pi^+\pi^-\pi^0$ was measured at VEPP-2M collider by SND detector in the energy range $2E_0=1.04-1.38$ GeV. The value of the cross section ~ 4 nb is in good agreement with previous measurements, but statistical accuracy is greatly improved. A broad peak with the mass $M_{vis} = 1220 \pm 20$ MeV, referred to as $\omega(1200)$ is seen. The fitting of the cross section by a sum Breit-Wigner resonances with the width not depending on energy, gives $\omega(1200)$ parameters, strongly depending on the interference phases choice. The PDG resonance $\omega(1420)$ is not seen in our fitting.

Acknowledgement. The authors express their gratitude for fruitful discussions to N.N.Achasov and A.E.Bondar.

This work is supported in part by STP ‘Integration’, grant No.274 and Russian Fund for Basic Researches, grants No. 96-15-96327, 97-02-18563 and 99-02-17155.

References

- [1] S.I.Dolinsky et al., Physics Reports V.202 (1991) 99.
- [2] A.Antonelli et al., Z.Phys. C56 (1992) 15.
- [3] Review of Particles Physics, The Eur. Phys. J. C 3, (1998).
- [4] M.N.Achasov et al., Nucl. Instr. Meth. A379 (1996) 505; A411 (1996) 337.
- [5] M.N.Achasov et al., Preprint Budker INP 98-65 Novosibirsk 1998.
- [6] A.V.Bozhenok et al., Nucl. Instr. Meth. A379 (1996) 505.
- [7] E.A.Kuraev, V.S.Fadin, Sov.J.Nucl.Phys. V.41 (1985) 466.
- [8] N.N.Achasov et al., Sov. J.Nucl. Phys. V.23 (1976) 610.
- [9] N.N.Achasov et al., Journ. of Mod. Phys. A7 (1992) 3187.

- [10] R.R.Akhmetshin et al., Physics Letters B434 (1998) 426.
- [11] R.R.Akhmetshin et al., Preprint Budker INP 99-11 Novosibirsk 1999.

Figure captions

- *Figure 1:* The visible cross section of the process $e^+e^- \rightarrow \pi^+\pi^-\pi^0$. The solid line shows the prediction of vector meson dominance model (VMD) for the processes (1) and (2).
- *Figure 2:* The detection efficiency of the process (2) versus radiative photon energy ω . At the low photon energy $\omega < 10$ MeV the value of the detection efficiency is the same as for the process (1).
- *Figure 3:* The $e^+e^- \rightarrow \pi^+\pi^-\pi^0$ total cross section, measured by VEPP-2M detectors ND [1], CMD-2 [10], and SND (this work). The only CMD-2 point at $2E=1040$ MeV with the cross section of 0.1 nb is not clearly seen, because it overlaps with the nearest SND point. The upper solid line is the result of fitting all existing experimental data according to Eq.6. The lower curve is a VMD model prediction.
- *Figure 4:* The cross section of the process $e^+e^- \rightarrow \pi^+\pi^-\pi^0$ from this work and DM2 [2] experiment. The upper solid line is the fit curve, obtained with Eq.6. The lower curve is a VMD model prediction.
- *Figure 5:* The cross section of the

process $e^+e^- \rightarrow \pi^+\pi^-\pi^0$, measured in different experiments in wide energy range. The solid curve corresponds to the best fit. The dashed line is a VMD model prediction.

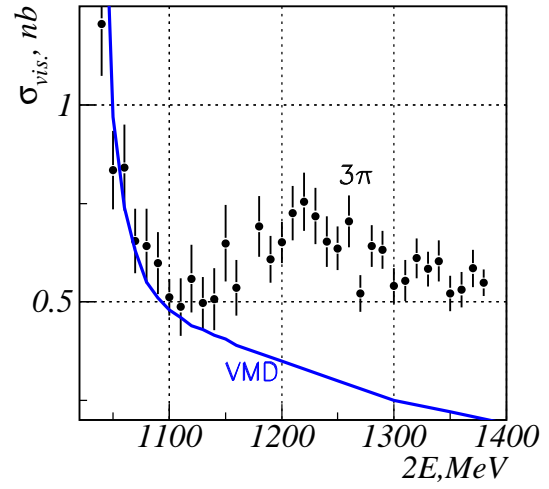


Figure 1: The visible cross section of the process $e^+e^- \rightarrow \pi^+\pi^-\pi^0$. The solid line shows the prediction of vector meson dominance model (VMD) for the processes (1) and (2).

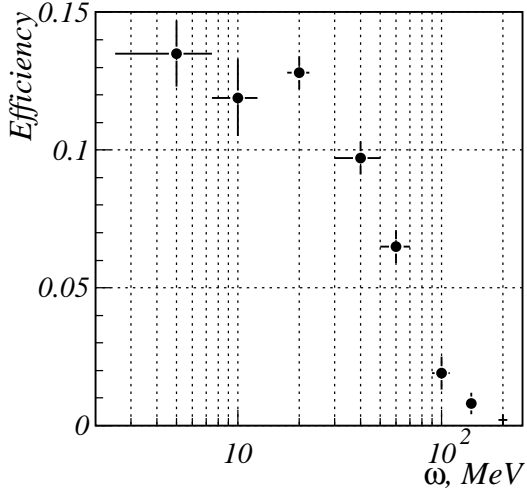


Figure 2: The detection efficiency of the process (2) versus radiative photon energy ω . At the low photon energy $\omega < 10$ MeV the value of the detection efficiency is the same as for the process (1)

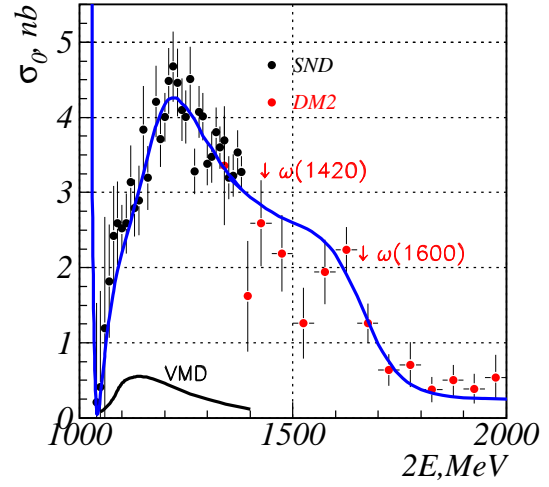


Figure 4: The cross section of the process $e^+e^- \rightarrow \pi^+\pi^-\pi^0$ from this work and DM2 [2] experiment. The upper solid line is the fit curve, obtained with Eq.6. The lower curve is a VMD model prediction.

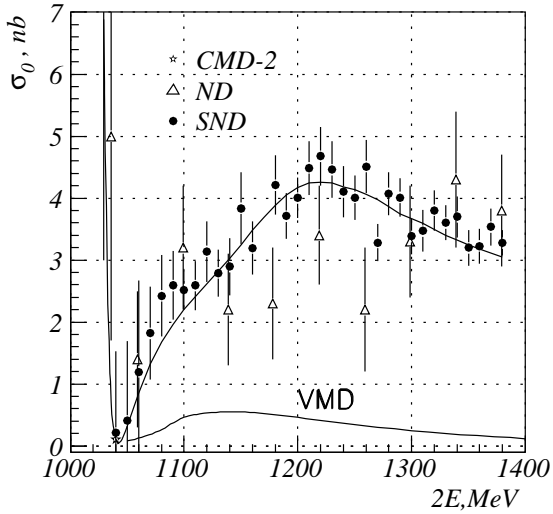


Figure 3: The $e^+e^- \rightarrow \pi^+\pi^-\pi^0$ total cross section, measured by VEPP-2M detectors ND [1], CMD-2 [10], and SND (this work). The only CMD-2 point at $2E=1040$ MeV with the cross section of 0.1 nb is not clearly seen, because it overlaps with the nearest SND point. The upper solid line is the result of fitting of all existing experimental data according to Eq.6. The lower curve is a VMD model prediction.

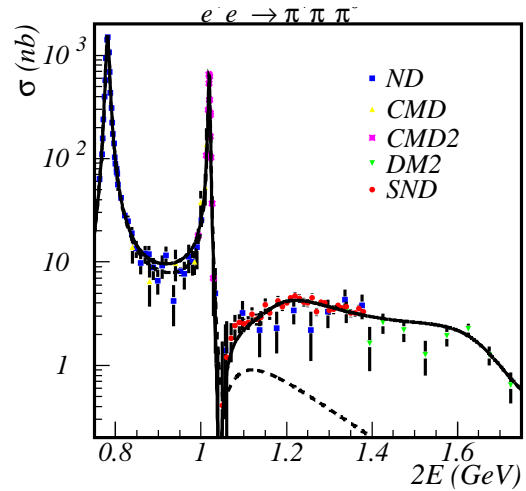


Figure 5: The cross section of the process $e^+e^- \rightarrow \pi^+\pi^-\pi^0$, measured in different experiments in wide energy range. The solid curve corresponds to the best fit. The dashed line is a VMD model prediction.

Table 1: The cross section σ_0 of $e^+e^- \rightarrow \pi^+\pi^-\pi^0$ process, measured in this work.

$2E_0$, MeV	σ_0 ,nb	$2E_0$, MeV	σ_0 ,nb
1040	0.2±1.3	1050	0.4±1.3
1060	1.2±1.5	1070	1.8±0.8
1080	2.5±0.7	1090	2.6±0.6
1100	2.5±0.3	1110	2.6±0.4
1120	3.1±0.5	1130	2.8±0.4
1140	2.9±0.5	1150	3.8±0.6
1160	3.2±0.4	1180	4.2±0.5
1190	3.7±0.4	1200	4.0±0.3
1210	4.5±0.4	1220	4.7±0.5
1230	4.5±0.5	1240	4.1±0.4
1250	4.0±0.4	1260	4.5±0.4
1270	3.3±0.3	1280	4.1±0.3
1290	4.0±0.3	1300	3.4±0.3
1310	3.5±0.3	1320	3.8±0.4
1330	3.6±0.3	1340	3.7±0.3
1350	3.2±0.3	1360	3.2±0.3
1370	3.5±0.4	1380	3.3±0.2

Table 2: The parameters of high mass ω -states, found in the fit, described by Eq.6 with phase option $\phi_{\omega(1200)} = \pi$ and $\phi_{\omega(1600)} = 0$

Parameter	$\omega(1200)$	$\omega(1600)$
M_{eff} , MeV	1170 ± 10	1643 ± 14
Γ_{eff} , MeV	187 ± 15	272 ± 29
σ_{max} ,nb	7.8 ± 0.2 ±1.0(<i>syst.</i>)	0.54 ± 0.13
$\Gamma_{\omega ee} \cdot B_{\omega 3\pi}$, eV	137 ± 3 ±15(<i>syst.</i>)	27 ± 7